Energy levels of isoelectronic impurities by large scale LDA calculations

Jingbo Li and Lin-Wang Wang
Lawrence Berkeley National Laboratory, Berkeley, California 94720
(Received 9 October 2002; published 22 January 2003)

Isoelectronic impurity states are localized states induced by stoichiometric single atom substitutions in bulk semiconductors. Photoluminescence spectra indicate deep impurity levels of 0.5–0.9 eV above the top of the valence band for such systems as GaN:As, GaN:P, CdS:Te, and ZnS:Te. Previous calculations based on small supercells seemingly confirmed these experimental results. However, the current *ab initio* calculations based on thousand-atom supercells indicate that the impurity levels of the above systems are actually much shallower (0.05–0.20 eV), and these impurity levels should be compared with photoluminescence excitation spectra, not photoluminescence spectra.

DOI: 10.1103/PhysRevB.67.033102 PACS number(s): 71.15.−m, 71.55.−i

An isoelectronic impurity atom has the same number of valence electrons as the host atom it replaces. For conventional alloys, such as $GaAs_xP_{1-x}$, a single-atom substitution will not cause a bound localized state. However, there is another class of alloys (unconventional), where a single-atom substitution will induce a localized electronic state. This often happens when the atomic sizes or the electronegativities of the substituting and the substituted atoms are sufficiently different.

Since Thomas and co-workers[1,2] identified a series of sharp lines in GaP:N and a broad fluorescence peak in CdS:Te (Ref. 3) more than 30 years ago, researchers have tried to understand the mechanism of such isoelectronic bound states. Various models have been proposed. Hopfield *et al.*[4] emphasized the different electronegativities between the isoelectronic impurity atom and the host atom. Depending on the increase or the decrease of the electronegativity, the bound state can be classified as a conduction-band-induced isoelectronic state (e.g., GaP:N and ZnTe:O) or valence-band-induced isoelectronic state (e.g., ZnS:Te and GaP:Bi). Allen[5] considered the lattice deformation due to different sizes of impurity atoms. This deformation causes a strain field effect that is related to the bulk deformation potential of the host. Phillips[6] further argued that the electron polarization and screening can also play an important role, which can significantly reduce the binding energy. More quantitatively, one can use the one-band one-site Koster-Slater model,[7] which uses the bulk one-band Green's function to describe the eigenvalue equation of the bound impurity state. Multiband models[8] have also been used to calculate these impurity states.

Besides model calculations, realistic numerical methods can also be used to study these systems. The traditional methods are the Green's-function methods[9] and parametrized tight-binding methods.[10] Recently, empirical pseudopotential methods (EPM's) and direct *ab initio* methods have become possible for such studies. An earlier calculation using EPM (Ref. 11) yielded GaN:As and GaN:P impurity levels as 0.75 and 0.61 eV, respectively, above the top of the valence band. These levels seem to agree well with the experimental photoluminescence (PL) results, which indicate corresponding levels of 0.91 and 0.59 eV above the top of the valence band. However, there are some uncertainties in the EPM calculation of impurity levels, since only binary systems are fitted in EPM. A more reliable way is to use the *ab initio* density-functional theory (DFT). A recent direct local-density approximation (LDA) calculation[12] using 64-atom cells has yielded shallower energy levels of 0.41 and 0.22 eV for GaN:As and GaN:P, respectively. Similarly, 64-atom cells have been used to calculate CdS:Te and ZnS:Te,[13] obtaining impurity levels of 0.19 and 0.29 eV, respectively, above the top of the valence band. All the above *ab initio* calculations use relatively small supercells (64 atoms), and obtain deep impurity levels. They seem to confirm a widely held belief that the valence-band-induced isoelectronic levels in such semiconductor systems are deep and strongly localized,[3,7,8] and the widely practiced 64-atom cell calculations are adequate.

In this work, we use newly available large-scale LDA methods to study the valence-band-induced isoelectronic levels in GaN:As, GaN:P, CdS:Te, and ZnS:Te of zinc-blende structures. Although the LDA is strictly valid only for systems in their ground state and underestimates the band gaps of semiconductors, it does describe the valence band accurately and has been used successfully to study valence-band-related electronic properties such as the band offsets.[14] Thus we believe it can be used to describe valence-band-induced impurity levels without further corrections. The challenge here is the large scale of the required calculations. Using supercells containing 512–4096 atoms, we show that the impurity energy levels are shallower than previously calculated results. Furthermore, they should be compared to experimental photoluminescence excitation (PLE) spectra, rather than the PL spectra. In contrast to what was previously believed, the impurity states are weakly localized, with their wave functions spreading outside the 64-atom cells. The relatively deep binding energies obtained in previous small cell calculations are artifacts caused by state-state couplings between neighboring impurities.

In this study we use a self-consistent LDA plane-wave pseudopotential method. We have used norm-conserving pseudopotentials. For Zn atoms we have included the d electrons in the valence band, but nonlinear core corrections are used for Ga and As. A 35-Ryd kinetic energy cutoff for the plane-wave basis set is used for GaN:As, GaN:P, and CdS:Te, while a 70-Ryd energy cutoff is used for ZnS:Te.

 ©2003 The American Physical Society

The LDA bulk lattice constants and bulk band structures agree well with the all-electron linear augmented plane-wave (LAPW) results.

While we have been able to calculate 512-atom systems directly for GaN:As, GaN:P, and CdS:Te using a parallel *ab initio* program,[15] to go beyond this supercell size is difficult. In order to calculate even larger systems, we have deployed a "charge patching method" (CPM).[16] In the CPM, the full self-consistent solution to the Kohn-Sham equations is calculated for a 64-atom supercell that contains an isoelectronic impurity at its center. The atomic positions within this 64-atom cell are relaxed using a valence force field (VFF) model. For a larger supercell with one impurity at the center, the previously calculated 64-atom cell charge density is used for the center cube, and the bulk charge density is used for the outer region. This generates the charge density $\rho(r)$ of the large supercell without doing self-consistent calculations. The potential $V(r)$ of this large system can then be calculated from $\rho(r)$ using the LDA formula. Next, the single-particle Schroedinger (Kohn-Sham) equation $H\psi_i=\epsilon_i\psi_i$ is solved using the folded spectrum method[17] for a few states near the band gap. This method changes the original equation into $(H-E_{ref})^2\psi_i=(\epsilon_i-E_{ref})^2\psi_i$ (where E_{ref} is an arbitrary energy inside the band gap) and uses energy minimization to solve the band edge ψ_i. For full details of the charge patching method, see Ref. 16.

Two aspects of the above procedure are worth checking. The first is the accuracy of the VFF model used for atomic relaxation within the 64-atom cell. To check this, we have relaxed the atoms in the 64-atom cell with full LDA forces and energies (to be called LDA relaxed). The second is the accuracy of the CPM. This includes the accuracy of the patched charge density and the fact that in CPM, the atoms outside the 64-atom cube are not relaxed, but are in their ideal zinc-blende positions. To test this, we have relaxed all the atoms in a 512-atom cell using VFF, then calculated the resulting system with a full self-consistent LDA method (to be called LDA-512VFF). A $2\times2\times2$ **k**-point grid is used for the 64-atom LDA calculations, and equivalently, 1 **k** point is used for the 512-atom LDA calculations. The eigenenergies given by these schemes are estimated to be within ~3 meV of those given by denser **k**-point sampling meshes.

Our results using the CPM method and the direct LDA method are summarized in Fig. 1 for the (a) GaN:As, (b) GaN:P, (c) CdS:Te, and (d) ZnS:Te systems. Shown in Fig. 1 is the single-particle impurity binding energy ε_b, defined as $\varepsilon_{im}-\varepsilon_{VBM}$ at the Γ point. Here, ε_{im} is the impurity eigenenergy, and ε_{VBM} is the bulk valence-band maximum (VBM), which is aligned by comparing $V(r)$ at the corner of the supercell with the bulk system. The impurity state has a t_2 symmetry, thus it has threefold degeneracy. Calculations have been performed for 64-, 512-, 1728-, and 4096-atom supercells.

In the 64-atom cells, the LDA-relaxed calculations (open triangles in Fig. 1) give almost the same (within 10 meV) ε_b as the VFF-relaxed calculations, indicating the adequacy of the VFF method. Furthermore, whether or not we fix the "surface atoms" of the 64-atom cubes makes practically no difference to ε_b (within 2 meV). The LDA-512VFF ε_b (filled triangles in Fig. 1) are smaller than the CPM results by about 58 meV for GaN:As, 33 meV for GaN:P, and 40 meV for CdS:Te. A major contribution of this energy difference is due to a "strain-relaxation" effect. When the outside atoms can be relaxed (as in LDA-512VFF), the 64-atom cube expands slightly. This lowers the level of the VBM. Since the impurity state consists mainly of host valence bands, and their amplitude is greatest within the 64-atom cube, the energy of the impurity state is also lowered. Although Fig. 1 shows some finite errors for the CPM procedure, we believe this CPM correction is additive upon larger systems, since the larger system should have basically the same atomic relaxation effects as for the 512-atom systems.

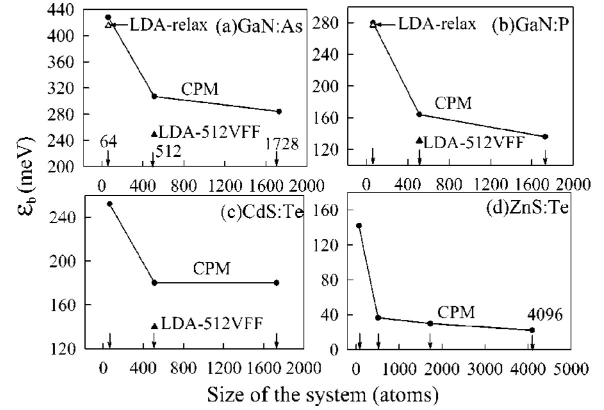

FIG. 1. Binding energies of (a) GaN:As, (b) GaN:P, (c) CdS:Te, and (d) ZnS:Te as functions of the size of the supercell. The vertical arrows indicate different supercell sizes. The eigenenergies are calculated at the Γ point.

A more quantitative way to estimate the strain effect is to calculate $\epsilon_{ave}=\int|\psi_{im}(r)|^2\epsilon(r)d^3r$, where $\psi_{im}(r)$ is the calculated impurity wave function (as will be shown in Fig. 2), and $\epsilon(r)$ is the local hydrostatic volume strain calculated from the VFF atomic positions as described in Ref. 18 (using the local natural bond length as the reference). Using

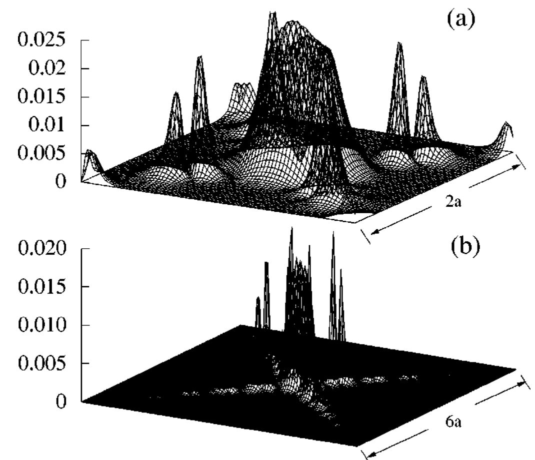

FIG. 2. Wave-function charge density of the impurity states of GaN:As at (001) cross sections. (a) 64-atom supercell contains one As impurity. (b) 1728-atom supercell contains one As impurity. The z-axis unit is 1/3 e/a.u.^{3}. a is the GaN lattice constant.

fully VFF relaxed 1728-atom systems, we get $\epsilon_{ave} = -0.053, -0.033, -0.023, -0.003$ for GaN:As, GaN:P, CdS:Te, and ZnS:Te, respectively. If the absolute deformation potentials are taken to be on the order of 1 eV,[19] then the corresponding strain effects in the impurity state energies are on the order of 50 meV.

The major effect shown in Fig. 1 is the significant decrease of the CPM-calculated ε_b from 64 atoms to 512 atoms. The ε_b more or less converges at 1728 atoms. It shows that the impurity states in these systems are indeed bound states, although not as strongly bound as previous calculations indicated. Note that, if the additional corrections to the CPM results are also taken into account as indicated in the LDA-512VFF of Fig. 1, the reduction of ε_b is even larger. Also note that, in the 64-atom cell calculations, our ε_b is similar to those reported in previous calculations.[12,13]

The increase in ε_b as the size of the system decreases can be partially explained as the coupling between neighboring impurity states in the small systems. The interaction of these states forms a bond wave function at the Γ point, which is high in energy for the valence bands, thus increasing the ε_b. To analyze this more quantitatively, we have calculated the energies at the X **k**-point $(\pi/2a,0,0)$ of the 64-atom cell, where a is the lattice constant. The impurity energies are lower than the Γ point results by 206, 238, 116, and 54 meV for GaN:As, CdS:Te, GaN:P, and ZnS:Te, respectively. These energy dispersions are on the same order as the energy drops in Fig. 1, confirming the fact that a large part of the energy drops in Fig. 1 is indeed due to the removal of the neighbor impurity state coupling. The interaction of these neighbor states can be further understood by looking at the wave functions.

Figure 2 plots wave functions of the impurity states in GaN:As for (a) the 64-atom cell and (b) the 1728-atom supercell. The impurity As atom is at the center of the cell box. In the 64-atom cell, strong peaks exist near the As site, as well as at the N atomic sites. It is difficult to tell whether or not this state is a bound state. Interactions between neighboring impurity states clearly exist, since significant peaks exist on the "cube surface" N atoms. In the 1728-atom large supercell, the localization of the impurity state becomes clear. It is a bound state, but with long-range tails in the (110) direction. In reciprocal space, one can project the impurity wave function into the host crystal bulk states at various **k** points. We find that for the 64-atom GaN:As cell, the impurity state has 50.3% at the Γ point, while that number drops to 5.2% for the 1728-atom cell. This is exactly how a localized state should behave.[20] We found similar behavior for all

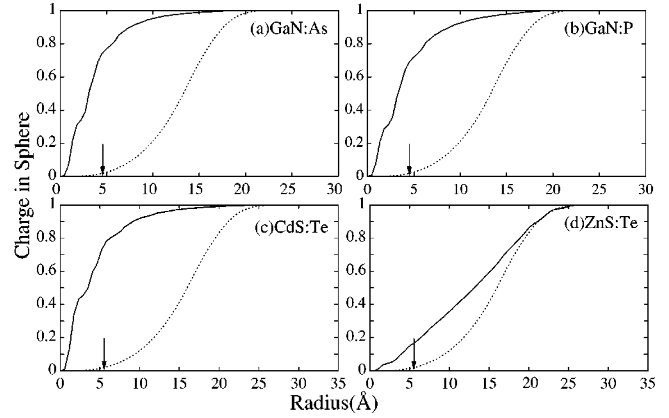

FIG. 3. Charge accumulation function $Q_i(R)$ of impurity states of (a) GaN:As, (b) GaN:P, (c) CdS:Te, and (d) ZnS:Te. R indicates the distance from the impurity atom. All the supercells contain 1728 atoms. The dotted curves show the uniform charge result. The arrows indicate the boundaries of the 64-atom cells.

the other impurity states shown in Fig. 1.

A more quantitative way to judge the real-space localization is to examine the "charge accumulation" function, defined as $Q_i(R)=\int_0^R|\Psi_i(R)|^2dR$, where R is a spherical radius centered at the impurity atom. Figure 3 shows the $Q_i(R)$ for the impurity states in GaN:As, GaN:P, CdS:Te, and ZnS:Te, all calculated from the 1728-atom supercells. The "charge accumulation" functions for uniform charge densities are also shown as dotted curves for comparison. From Fig. 3, we can make the following observations: (i) The solid curves approach 1 faster than the dotted curves, indicating localization in real space. (ii) GaN:As has the strongest localization, and ZnS:Te has the weakest. This is in agreement with the converged binding energies shown in Fig. 1. (iii) At the boundary of the 64-atom cell (indicated by the vertical arrows in Fig. 3), $Q_i(R)$ is only about 16% to 78%. That means, for the converged wave functions, depending on the case, 22–84 % of the wave function charge density is outside the 64-atom cell. Thus the 64-atom cell is not large enough, and these impurity states are only weakly localized.

We now compare our calculated single-particle impurity binding energy ε_b with the optical measurements. We have listed our calculated ε_b in the fifth column of Table I. Note that, to get the best estimate of our calculated ε_b, we have taken into account the CPM corrections discussed above, and added that to the converged CPM energies shown in Fig. 1.[21] We have also listed the available optical measurements in Table I.[22–25] The experimental situations for these systems

TABLE I. Experimental data for GaN:As (Refs. 20 and 21), GaN:P (Refs. 20 and 21), CdS:Te (Ref. 22), and ZnS:Te (Ref. 23) of binding energy ε_b defined by PL, ZPL, and PLE energies and the bulk band gap E_g. The data in fifth column are the present LDA calculations with large supercells. The unit of energy is eV.

Material	$\varepsilon_b(E_g\text{-PL})$	$\varepsilon_b(E_g\text{-ZPL})$	$\varepsilon_b(E_g\text{-PLE})$	ε_b (present calc.)
GaN:As	0.91	0.287	unknown	0.226
GaN:P	0.59	0.232	unknown	0.103
CdS:Te	0.48	0.22	0.092	0.14
ZnS:Te	0.65	0.4	0.09	0.04

are far from perfect. For example, there are problems of impurity concentration estimation, peak identification, and clustering effects. Nevertheless, a few experiments have been carried out for these systems, especially for their optical spectra. The most reliable optical signal is the PL spectra. However, unlike the conduction-band-induced isoelectronic states, for the valence-band-induced isoelectronic states studied here, even for relatively small impurity concentrations ($2\times10^{18}/\mathrm{cm}^3$), one finds a broad PL spectra peak (a few tenths of an eV).[24] This indicates strong electron-phonon coupling. For all these systems, there are experimental estimates of the zero-phonon lines (ZPL's). For CdSe:Te and ZnS:Te, there are also experimental estimates of PLE energies caused by the impurity states, though the accuracy of these estimates is not as good as for PL. Note that the ZPL and PL can differ by a few tenths of an eV. In previous work,[11–13] the calculated ε_b have been compared to the experimental PL (Refs. 11 and 13) and ZPL (Ref. 12) values. Given the large difference between the PL, ZPL, and PLE values, a more careful analysis is needed here. Our $E_g-\varepsilon_b$ is very close to the total-energy difference $E_{excited}-E_{ground}$, where $E_{excited}$ is a LDA total energy calculated under a self-consistent constraint LDA approach: one impurity state is unoccupied, one of the lowest conduction-band states is occupied, and the same atomic positions are used as in E_{ground}. For example, for ZnS:Te, $E_{excited}-E_{ground}$ and $E_g-\varepsilon_b$ differ by only 4 meV in a 64-atom calculation. In a Franck-Condon picture[24,25] as shown in Fig. 4, the above $E_{excited}$ and E_{ground} have the same "configuration coordinate Q," thus $E_{excited}-E_{ground}$ should correspond to the PLE. Hence here our calculated ε_b should be compared with the experimental PLE, not the PL or ZPL values. In this regard, our calculated results agree well with the experimental results. Although the experimental PLE's for GaN:As and GaN:P are not known, our ε_b is smaller than the experimental E_g-ZPL, consistent with our argument.

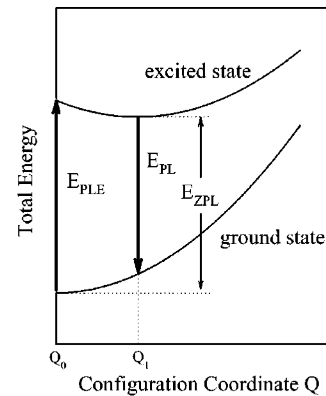

FIG. 4. Configuration coordinate diagram for LDA total-energy calculation. The configuration coordinate Q is an overall description for the atomic position of the system.

In summary, we have reported the electronic structures of valence-band-induced isoelectronic levels in III-V and II-VI semiconductors. We found that (i) the widely used 64-atom unit-cell calculations are not converged and there is a strong coupling between neighboring impurity states; (ii) the current ideas regarding these impurity states as strongly localized deep impurity states are inappropriate; the binding energies of these impurity states are in the range of 50–200 meV, not in the range of 500–900 meV; and (iii) the calculated impurity eigenenergies should be compared with experimental PLE results, not PL results.

This work was supported by the U.S. Department of Energy, OER-BES, under contract No. DE-AC03-76SF00098. This research used the resources of the National Energy Research Scientific Computing Center, which is supported by the Office of Science of the U.S. Department of Energy.

[1] D. G. Thomas, J. J. Hopfield, and C. J. Frosch, Phys. Rev. Lett. **15**, 857 (1965).
[2] D. G. Thomas and J. J. Hopfield, Phys. Rev. **150**, 680 (1966).
[3] J. D. Cuthbert and D. G. Thomas, J. Appl. Phys. **39**, 1573 (1968).
[4] J. J. Hopfield, D. G. Thomas, and R. T. Lynch, Phys. Rev. Lett. **17**, 312 (1966).
[5] W. G. Allen, J. Phys. C **1**, 1136 (1968); **4**, 1936 (1971).
[6] J. C. Phillips, Phys. Rev. Lett. **22**, 285 (1969).
[7] R. A. Faulkner, Phys. Rev. **175**, 991 (1968).
[8] K. P. Tchakpele and J. P. Albert, Phys. Status Solidi B **149**, 641 (1988).
[9] An-Ban Chen and B. Segall, Phys. Rev. B **12**, 600 (1975).
[10] An-Ban Chen and A. Sher, Phys. Rev. B **22**, 3886 (1980).
[11] L. Bellaiche, S. H. Wei, and A. Zunger, Phys. Rev. B **54**, 17 568 (1996); Appl. Phys. Lett. **70**, 3558 (1997).
[12] T. Mattila and A. Zunger, Phys. Rev. B **58**, 1367 (1998).
[13] S.-H. Wei, S. B. Zhang, and A. Zunger, J. Appl. Phys. **87**, 1304 (2000).
[14] S.-H. Wei and A. Zunger, Appl. Phys. Lett. **72**, 2011 (1998).
[15] http://www.nersc.gov/~linwang/PEtot/PEtot.html
[16] L. W. Wang, Appl. Phys. Lett. **78**, 1565 (2001).
[17] L. W. Wang and A. Zunger, J. Chem. Phys. **100**, 2394 (1994).
[18] C. Pryor, J. Kim, L. W. Wang, A. J. Williamson, and A. Zunger, J. Appl. Phys. **83**, 2548 (1998).
[19] S.-H. Wei and A. Zunger, Phys. Rev. B **60**, 5404 (1999).
[20] L. W. Wang, L. Bellaiche, S. H. Wei, and A. Zunger, Phys. Rev. Lett. **80**, 4725 (1998).
[21] For ZnS:Te, we are unable to calculate the 512-atom system. However, we estimate that its "strain-relaxation" correction to CPM is small, since its wave function spreads out to the whole 512-atom unit cell. Besides, the spin-orbit interaction effect is included in this system, which increases ε_b by about 10 meV.
[22] W. M. Jadwisienczak and H. J. Lozykowski, in *Nitride Semiconductors*, edited by F.A. Ponce, S.P. DenBaars, B.K. Meyer, S. Nakamura, and S. Strite, MRS Symposia Proceedings No. 482 (Materials Research Society, Pittsburgh, 1998), p. 1033.
[23] J. I. Pankove and J. A. Hutchby, J. Appl. Phys. **47**, 5387 (1976).
[24] D. M. Roessler, J. Appl. Phys. **11**, 4589 (1970).
[25] T. Fukushima and S. Shionoya, Jpn. J. Appl. Phys., Part 1 **12**, 549 (1973).